BEC BIOENERGETICS COMMUNICATIONS Bioenerg Commun 2021.4 doi:10.26124/bec:2021-0004
Open Access

Technical | Experimental Communication

Cite
Komlódi T, Sobotka O, Gnaiger E (2021) Facts and artefacts on the oxygen dependence of hydrogen peroxide production using Amplex UltraRed. Bioenerg Commun 2021.4. doi:10.26124/bec:2021-0004

Author contributions
EG and OS designed the work; OS and TK collected data; OS and TK analyzed data; TK, OS, and EG wrote and revised the article.

Conflicts of interest
EG is founder and CEO of Oroboros Instruments, Innsbruck, Austria.

Academic editor
Andrew Murray, Department of Physiology, Development & Neuroscience, University of Cambridge, UK

Copy editor
Lisa Tindle-Solomon

Received 2021-11-09
Reviewed 2021-12-15
Resubmitted 2021-12-17
Accepted 2021-12-17

Published 2021-12-21

Editorial and peer review record
doi.org/10.26124/bec:2021-0004

Preprint
MitoFit Preprints 2021.10
doi:10.26124/mitofit:2021-0010

Data availability
Original files are available Open Access at Zenodo repository: 10.5281/zenodo.5785626

Facts and artefacts on the oxygen dependence of hydrogen peroxide production using Amplex UltraRed

Timea Komlódi[1#], Ondrej Sobotka[2#], Erich Gnaiger[1*]

[1] Oroboros Instruments, Innsbruck, Austria
[2] 3rd Department of Internal Medicine – Metabolic Care and Gerontology, University Hospital Hradec Kralove, Department of Physiology, Faculty of Medicine in Hradec Kralove, Charles University, Czech Republic

[#] Shared first authors
[*] Corresponding author: erich.gnaiger@oroboros.at

Abstract

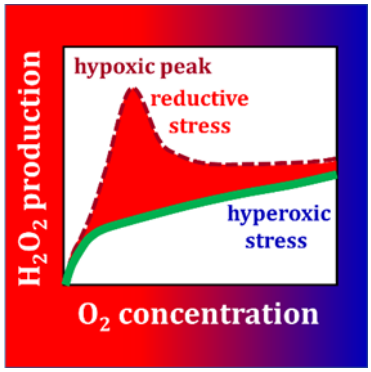

The fluorometric Amplex™ UltraRed AmR assay is frequently used for quantitative assessment of hydrogen peroxide production. It is specific to H_2O_2, can be calibrated accurately, and allows continuous real-time measurement. Without correction for the background fluorescence slope, however, H_2O_2-independent formation of the fluorescent product UltroxRed (or resorufin from Amplex™ Red) leads to artefacts.

We analysed (*1*) the medium specificity of the background fluorescence slope of the AmR assay, and (*2*) the oxygen dependence of H_2O_2 flux in baker´s yeast *Saccharomyces cerevisiae*. Apparent H_2O_2 flux, O_2 concentration, and O_2 flux were measured simultaneously by high-resolution respirometry equipped with the fluorescence module. The apparent H_2O_2 flux of yeast showed a maximum under hypoxia when incubated in Dulbecco´s Phosphate Buffered Saline DPBS or KCl-medium. This hypoxic peak

Keywords

Amplex UltraRed, AmR
Amplex UltroxRed, xRed
hydrogen peroxide production
H_2O_2 flux
respiration media
mitochondrial respiration medium 5, MiR05
yeast
oxygen dependence
reductive stress
anoxia
hypoxia
O_2 kinetics
respiration
reoxygenation

increased with the sequential number of normoxic-anoxic transitions. Even in the absence of yeast, the fluorescence slope increased at low O_2 levels as a function of fluorescence intensity. The hypoxic peak was not observed in mitochondrial respiration medium MiR05. Therefore, the hypoxic peak was a medium-specific background effect unrelated to cell physiology. In MiR05, H_2O_2 production of yeast decreased linearly from hyperoxia to hypoxia, with a steep decline towards anoxia. Respiration and oxygen dependence expressed as p_{50} of yeast were higher in MiR05 than DPBS. Respiration was a hyperbolic function of oxygen concentration in the low-oxygen range. The flux-dependence of oxygen affinity explained the higher p_{50} in MiR05.

1. Introduction

The formation of reactive oxygen species ROS is an inevitable side effect of aerobic respiration (Skulachev 1996). ROS involve several chemical species of reactive molecules derived from oxygen in redox reactions including photo- and chemiexcitation (Sies and Jones 2020). Physiologically, ROS play a vital role in many redox signaling processes such as differentiation and apoptosis (Brand 2016; Buettner et al 2013). The imbalance between generation and removal of ROS via the antioxidant systems leads to *oxidative stress*, which is accompanied by damage of proteins, lipids and nucleotides, disturbance of cell metabolism, and derangement of ROS signaling (Paniker 1970; Sies 1997; Xiao and Loscalzo 2020). According to the concept of *reductive stress*, reduced compounds — e.g. NAD(P)H and glutathione — accumulate at low oxygen levels causing high ROS production under hypoxia, inducing hypoxic ROS stress and disturbing redox homeostasis (Aon 2010; Dawson et al 1993; Korge et al 2015; Xiao and Loscalzo 2020). In contrast, hyperoxic conditions induce oxidative stress driven by high concentrations of oxygen as a substrate for ROS production (Ottolenghi et al 2020).

Quantification of ROS species is challenging due to their short lifetime, ranging from nanoseconds to seconds. An ideal probe for ROS measurement (*1*) reacts rapidly with ROS to outcompete the cellular antioxidant systems, (*2*) produces a stable, measurable, and quantifiable product, (*3*) is specific to a particular ROS species, and (*4*) has sufficiently high sensitivity (Dikalov and Harrison 2014). Measurement of changes in fluorescence caused by oxidation of molecular probes provides a convenient way for determination of ROS production. Most popular assays for determination of ROS production are based on Amplex™ UltraRed (AmR), dihydroethidine (DHE), and 2′,7′-dichlorofluorescin diacetate (DCFH-DA).

The AmR assay is one of the most frequently applied methods for assessing H_2O_2 production. H_2O_2 is the most stable form of ROS. AmR reacts with H_2O_2 catalyzed by horseradish peroxidase HRP, forming the fluorescent product resorufin Res in the case of

Amplex™ Red or UltroxRed (xRed) in the case of Amplex™ UltraRed. Superoxide dismutase SOD converts superoxide to H_2O_2 which can freely cross biological membranes (Bienert et al 2006). According to Mohanty et al (1997) AmR does not cross biological membranes, whereas other studies suggest the contrary (Miwa et al 2015). Benefits of this method are (*1*) the high sensitivity towards H_2O_2 (Mishin et al 2010; Tretter and Ambrus 2014) compared to DCFH-DA (Dikalov and Harrison 2014; Kalyanaraman et al 2012; Mohanty et al 1997), (*2*) the simple and accurate calibration of the fluorescence signal using H_2O_2, since the fluorescence signal (i.e. fluorescence intensity) is a linear function of added H_2O_2 concentrations up to 5 µM (Tretter and Ambrus 2014) or up to 3 µM resorufin (Krumschnabel et al 2015), (*3*) the low inhibitory effect on mitochondrial (mt) respiration compared to other fluorescence dyes used in studies of bioenergetics, e.g. safranin (Makrecka-Kuka et al 2015), and (*4*) instantaneous consumption of H_2O_2 (less than 5-10 s; Tretter and Ambrus 2014) which makes this probe an ideal candidate for real-time and continuous measurement of H_2O_2 production. Disadvantages of the AmR assay are that the fluorescent product Res or xRed may be formed by H_2O_2-independent side reactions. These side reactions can be measured as the increase over time (slope) of background fluorescence intensity in the absence of sample without addition of H_2O_2: (*1*) in the absence of HRP during photooxidation of AmR upon light exposure (Zhao et al 2012), and (*2*) in the presence of HRP as spontaneous autooxidation of AmR (Zhou et al 1997). The components of the respiration medium exert an effect on the background fluorescence slope and thus influence the H_2O_2-sensitivity of the AmR assay (Krumschnabel et al 2015; Komlódi et al 2018).

In the present study, we investigated in various respiration media (*1*) the background fluorescence slope of the AmR assay at different O_2 concentrations, and (*2*) the O_2 dependence of the apparent H_2O_2 flux in yeast cells used as a model system.

2. Materials and methods

2.1. Reagents

All chemicals were purchased from Sigma Aldrich (Carlsbad, CA, US) with exception of diethylenetriamine-*N*,*N*,*N*',*N*'',*N*'''-pentaacetic acid DTPA (Dr. Ehrenstorfer GmbH; Augsburg, Germany), Amplex™ UltraRed and Dulbecco´s Phosphate-Buffered Saline DPBS (Thermo Fisher Scientific, Waltham, MA, US). MiR05-Kit (Oroboros Instruments, Innsbruck, Austria), DPBS and KCl-based respiration medium were used for simultaneous high-resolution respirometry HRR and fluorescence measurements. Components of respiration media are listed in Table 1.

2.2. Yeast preparation

Commercially available freeze-dried baker's yeast (*Saccharomyces cerevisiae*) was rehydrated in Na-phosphate buffer (50 mM Na_3PO_4; pH 7.1) at a concentration 20 mg/mL at 30 °C to 40 °C preserving high viability (Crowe et al 1998; Koga et al 1966). To avoid cell sedimentation and clumping, the yeast suspension was pipetted 20-times slowly and 10-times fast up and down in a 2-mL Eppendorf tube using a 1-mL pipette. Immediately

afterwards, 20 µL yeast suspension was injected with a 50-µL Hamilton syringe into the O2k-chamber through the titration capillary of the stopper. The experimental concentration of yeast was 0.2 mg/mL unless otherwise stated. Independent preparations are indicated as separate experimental days in the figure legends.

2.3. High-resolution respirometry

O_2 concentration and xRed fluorescence were measured simultaneously using the O2k-FluoRespirometer (Oroboros Instruments, Innsbruck, Austria). The Oroboros O2k continuously monitors the O_2 concentration and plots in real-time the O_2 consumption of the biological sample. The O2k consists of two instrumental chambers which are designed to perform unlimited titrations during the experimental assay. All experiments were performed under constant stirring (750 rpm) in pre-calibrated 2-mL chambers. Polarographic oxygen sensor POS tests including air calibration (every experimental day) and monthly instrumental O_2 background tests including zero calibration of the POS were performed routinely as instrumental quality control (Doerrier et al 2018; Gnaiger 2001; 2008). The oxygen solubility of the medium at 37 °C was 9.72 µM/kPa for conversion of partial pressure to O_2 concentration equivalent to the O_2 solubility factor of 0.92. The volume-specific oxygen flux $J_{V,O2}$ was calculated as the negative time derivative of the O_2 concentration by DatLab 7.4. The O_2 flux was corrected for instrumental O_2 background flux $J°_{O2}$.

Sequential anoxia-reoxygenation cycles were performed to measure ROUTINE respiration in DPBS, KCl-medium or MiR05 without addition of external fuel substrates. Reoxygenations were performed by opening the chamber to the stopper-spacer position to obtain a well-defined gas phase above the aqueous phase ('open' chamber). To decrease the O_2 concentration, nitrogen gas was injected with a 60-mL syringe into the gas phase obtained in the open chamber. The chambers were closed when approaching the required O_2 level.

Table 1. Composition of respiration media with concentrations [mM]. DPBS: Dulbecco's Phosphate-Buffered Saline; MiR05 (Gnaiger et al 2000); KCl-medium (Hoffman et al 2007).

	MiR05	DPBS	KCl-medium
sucrose	110	-	25
K-lactobionate	60	-	-
K-HEPES	20	-	-
taurine	20	-	-
KCl	-	2.68	125
K_2HPO_4	10	1.42	5
$MgCl_2$	3	-	5
NaCl	-	136.89	-
$Na_2HPO_4 \cdot 7H_2O$	-	8.06	-
EGTA	0.5	-	-
BSA [mg/mL]	1	-	0.5
pH	7.1 (KOH; 30 °C)	7.0-7.3 (KOH, HCl; 24 °C)	7.4 (KOH, HCl; 24 °C)

2.4. Oxygen kinetics

Oxygen kinetics is assessed in a closed chamber during normoxic-anoxic transitions when the O_2 concentration decreases to zero (Gnaiger et al 1995; Gnaiger 2001). The oxygen concentration at which O_2 flux is reduced to 50 % is the kinetic parameter c_{50} [µM] or p_{50} [kPa] calculated from the hyperbolic fit comparable to Michaelis-Menten kinetics. The maximum enzyme reaction velocity V_{max} at saturating substrate concentration corresponds to pathway flux J_{max} in mitochondria or cells. Oxygen kinetics was measured in freeze-dried baker´s yeast in DPBS and MiR05 at 37 °C in the ROUTINE state without exogenous substrates. Importantly, $J_{V,O2}$ was corrected for instrumental O_2 background. Zero oxygen calibrations were obtained after normoxic-anoxic transitions. The first-order exponential time constant τ of the POS was determined by stirrer tests at τ = 2.9 s for signal deconvolution (Gnaiger 2001). The data recording interval of 2 s was sufficient for resolution of O_2 kinetics at low O_2 affinity of yeast cells. Calculations were performed automatically by an O_2 kinetics software (Oroboros Instruments; Doerrier et al 2018).

2.5. Hydrogen peroxide flux

Fluorescence was measured using Smart Fluo-Sensors Green (Oroboros Instruments; excitation 525 nm, emission ~600 nm). The optical sensors were inserted through the front window of the O2k-chambers. Horseradish peroxidase HRP (1 U/mL) and superoxide dismutase SOD (5 U/mL) were titrated into the chamber before Amplex™ UltraRed AmR (10 µM). The iron chelator DTPA (15 µM) was applied to decrease the background fluorescence slope of the AmR assay (Komlódi et al 2018). DPBS(+), KCl-medium(+), and MiR05(+) contained DTPA; DPBS(-), KCl-medium(-), and MiR05(-) did not contain DTPA. The excitation light intensity was set at 500 mV except when indicated otherwise.

AmR reacts with H_2O_2 forming the fluorescent dye xRed. The fluorescence intensity (proportional to the fluorescence signal) emitted in the AmR assay was calibrated by 0.1-µM H_2O_2 titrations. At a gain setting of 1000, the amperometric raw signal of 1 µA is converted to 1 V. Multiple H_2O_2 calibrations were performed at different states of the protocol to quantify the sensitivity of the AmR assay over time and experimental conditions (Komlódi et al 2018). The fluorescence slope is calculated as the non-linear time derivate of the fluorescence signal by DatLab 7.4.

2.6. Background fluorescence slope at air saturation

In contrast to an instrumental background effect, the chemical background fluorescence slope of the AmR assay increased over time in DPBS and KCl-medium at constant normoxic O_2 concentration near air saturation (~180 µM; Figure 1a and b). The background fluorescence slope showed deviations from linearity above ~5-6 µA fluorescence intensity in DPBS and KCl-medium. This can be explained by (*1*) the decreasing concentration of available AmR, and (*2*) the accumulation of xRed (or Res) over the course of the experiment leading to allosteric inhibition of HRP (Piwonski et al 2012). In MiR05, however, a moderate and linear increase was observed of the

background fluorescence slope over time (Figure 1c). The background fluorescence slope $J_{amp,BGr}$ [nA·s^{-1}] was a hyperbolic function of fluorescence intensity I_{amp} in KCl-medium (Figure 1d) but a linear function of I_{amp} in MiR05 with slope b_{amp} and intercept a_{amp} (Figure 1e),

MiR05: $$J_{amp,BGr} = b_{amp} \cdot I_{amp} + a_{amp}$$ Eq.1

b_{amp} and a_{amp} were determined for each Lot of MiR05-Kit (Table 2).

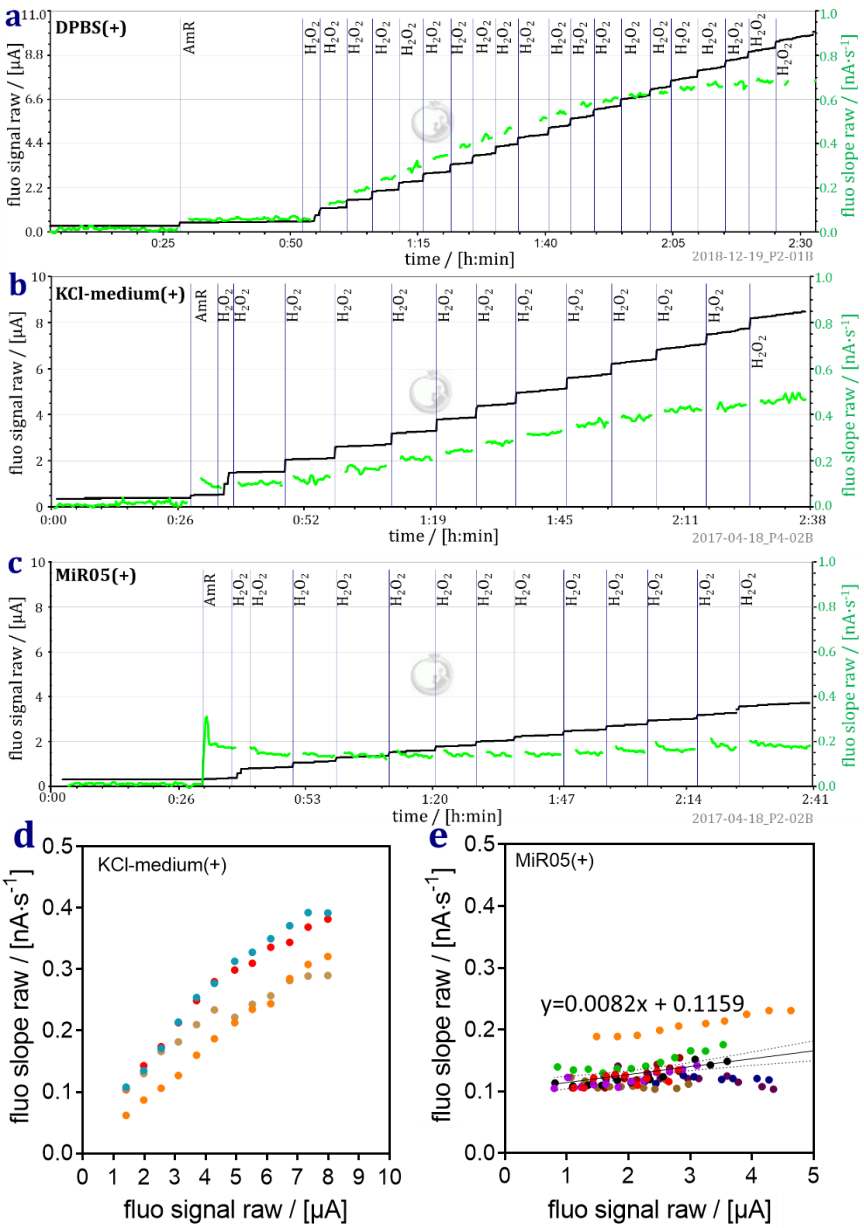

Figure 1. Background fluorescence slope in the Amplex™ UltraRed assay in different respiration media at constant O_2 concentration near air saturation (~170-180 µM) in the presence of DTPA **(+)**. **(a)** DPBS; **(b)** KCl-medium; **(c)** MiR05 (Lot#0915). Black plots: background fluorescence signal related to fluorescence intensity [µA]; green plots: background fluorescence slope [nA·s^{-1}]. Background fluorescence slope [nA·s^{-1}] as a function of fluorescence signal [µA] in **(d)** KCl-medium (technical repeats, n=4) and **(e)** MiR05 (Lot#0915; technical repeats, n=9); each colour represents a separate experiment.

3. Results

Respiration (Figure 2a-c) and xRed fluorescence (Figure 2d-i) were measured in a sequence of normoxic-anoxic transitions. When rehydrated, freeze-dried yeast rapidly

restored active metabolism (Crowe et al 1998). In DPBS and KCl-medium the apparent H_2O_2 flux increased with decreasing O_2 concentration resulting in a *hypoxic peak* of the fluorescence slope before it declined towards anoxia (Figure 2d and e). The hypoxic peak became increasingly prominent following each reoxygenation after anoxia. In MiR05, however, the hypoxic peak was not observed, but the apparent H_2O_2 flux declined continuously with decreasing O_2 concentration in a biphasic kinetic O_2 dependence (Figure 2f). How can these contradictory observations be explained? Is the hypoxic peak related to acclimatization to O_2 availability and O_2 sensing of yeast in different buffers, or is it the result of a methodological artefact due to the interplay between respiration medium and the AmR assay?

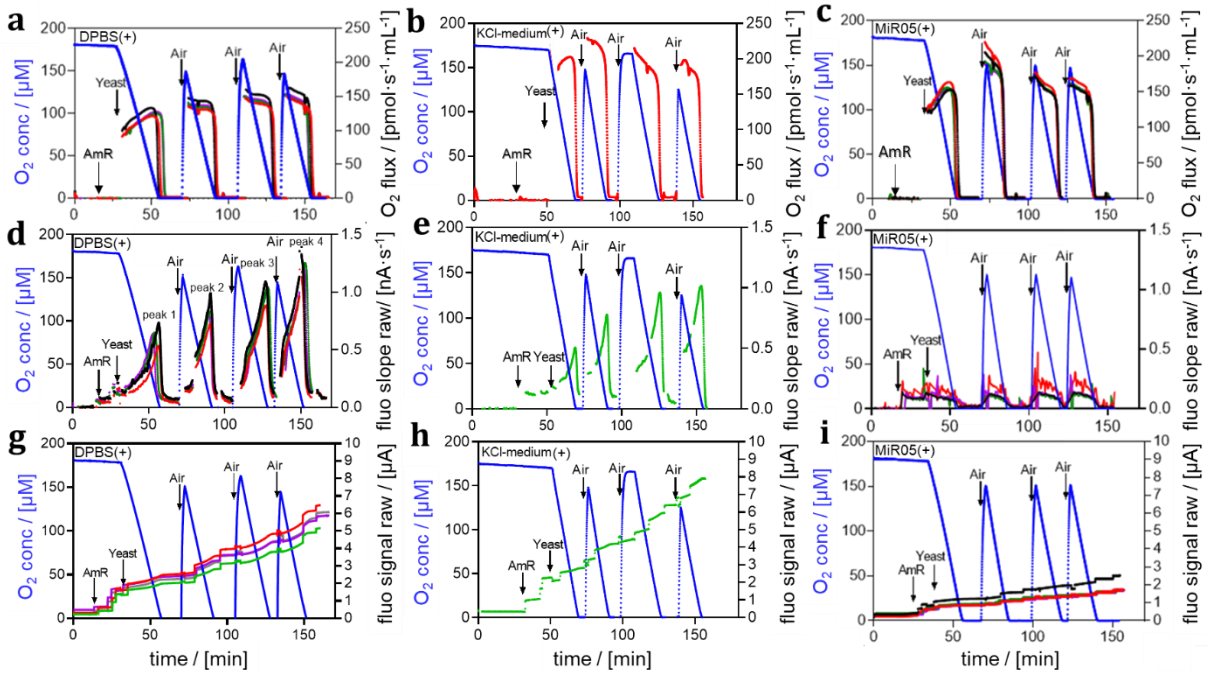

Figure 2. Amplex™ UltraRed assay and high-resolution respirometry in repeated normoxic-anoxic transitions in yeast measured in DPBS(+) (a, d, g), KCl-medium(+) (b, e, h), and MiR05(+) (c, f, i) with DTPA. Blue plots: O_2 concentration [µM] decreasing due to respiration; brief periods of anoxia were followed by reoxygenations. **(a, b, c)** Volume-specific O_2 flux [pmol·s^{-1}·mL^{-1}]; **(d, e, f)** non-calibrated fluorescence slope (raw) [nA·s^{-1}]; **(g, h, i)** non-calibrated (raw) fluorescence signal (proportional to fluorescence intensity) [µA]. One representative trace **(b, e, h)** or technical repeats (*n*=4) recorded in parallel in four different chambers **(a, c, d, f, g, i)**. Experiments DPBS and MiR05: 2018-12-06_P3-02, 2018-12-06_P4-02, 2018-12-06_P1-01, 2018-12-06_P2-01, KCl-medium: 2017-04-18_P7-02A.

3.1. Hypoxic H_2O_2 peak: fact or artefact?

The fluorescence signal increases over time owing to the accumulation of xRed originating from AmR due to (*1*) titrations of H_2O_2 during assay calibrations, (*2*) extracellular H_2O_2 flux by yeast, and (*3*) artificial H_2O_2-independent increase of background fluorescence (Figure 2g-i). To elucidate the origin of the hypoxic peak in

DPBS and KCl-medium, we analysed the effect of fluorescence intensity (proportional to the fluorescence signal) on the apparent H_2O_2 flux. To differentiate between the effects of the O_2 regime and exposure time on H_2O_2 production by yeast and the effect of fluorescence intensity, we performed parallel experiments: the control group (C) with initial titration of AmR before adding yeast cells, and the experimental group (E) with delayed addition of AmR to yeast cells (Figure 3).

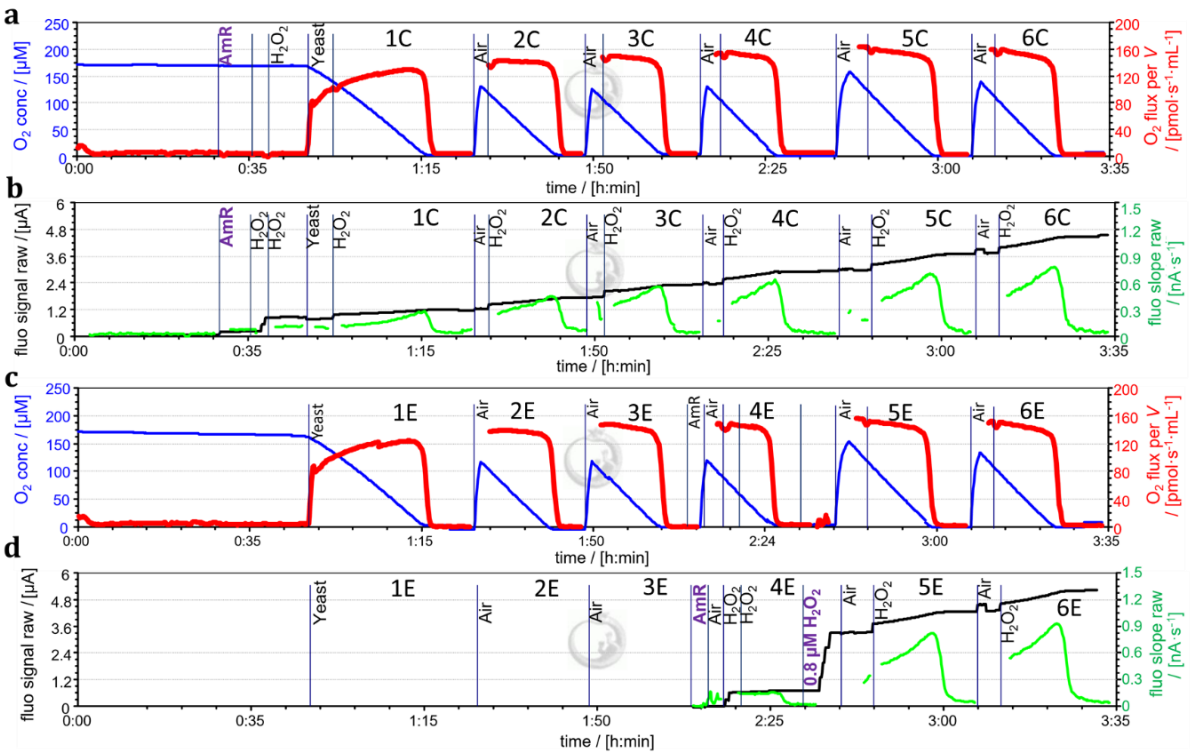

Figure 3. Effect of accumulating concentrations of xRed on the hypoxic peak of the fluorescence slopes in repeated normoxic-anoxic transitions in yeast incubated in DPBS(+) containing DTPA. Blue plots: O_2 concentration [µM] decreasing due to respiration; brief periods of anoxia were followed by reoxygenation. Red plots: volume-specific O_2 flux [pmol·s^{-1}·mL^{-1}]; black plots: non-calibrated fluorescence signal (proportional to fluorescence intensity) [µA]; green plots: non-calibrated (raw) fluorescence slope [nA·s^{-1}]. 1C to 6C and 1E to 6E: normoxic-anoxic transitions. **(a, b)** Control: AmR titrated before addition of yeast; **(c, d)** Experimental group: AmR titrated immediately before 4E. The fluorescence intensity was increased by titration of 0.8 µM H_2O_2 before 5E. Experiment 2018-12-19 P8-02.

Consistent with results shown in Figure 2d and e, the hypoxic peak was observed during the normoxic-anoxic transitions and increased after each sequential reoxygenation in the controls (1C to 6C; Figure 3a and b). The hypoxic peak 4C was already highly pronounced. When AmR was not added at the start but only before transition 4E in the experimental group, however, the hypoxic peak 4E was comparable or even less pronounced than the hypoxic peak 1C in the control (Figure 3). Before transition 5E, titration of 0.8 µM H_2O_2 increased the fluorescence intensity which resulted

in a hypoxic peak 5E of the same extent as 5C in the control. Importantly, O_2 flux did not differ between the two parallel experimental regimes using yeast from the same batch (Figure 3a and c). These results suggest that the hypoxic peak observed in DPBS at low O_2 concentration was related to artificial background fluorescence intensity in contrast to a redox response of yeast cells as acclimatization to the O_2 regime.

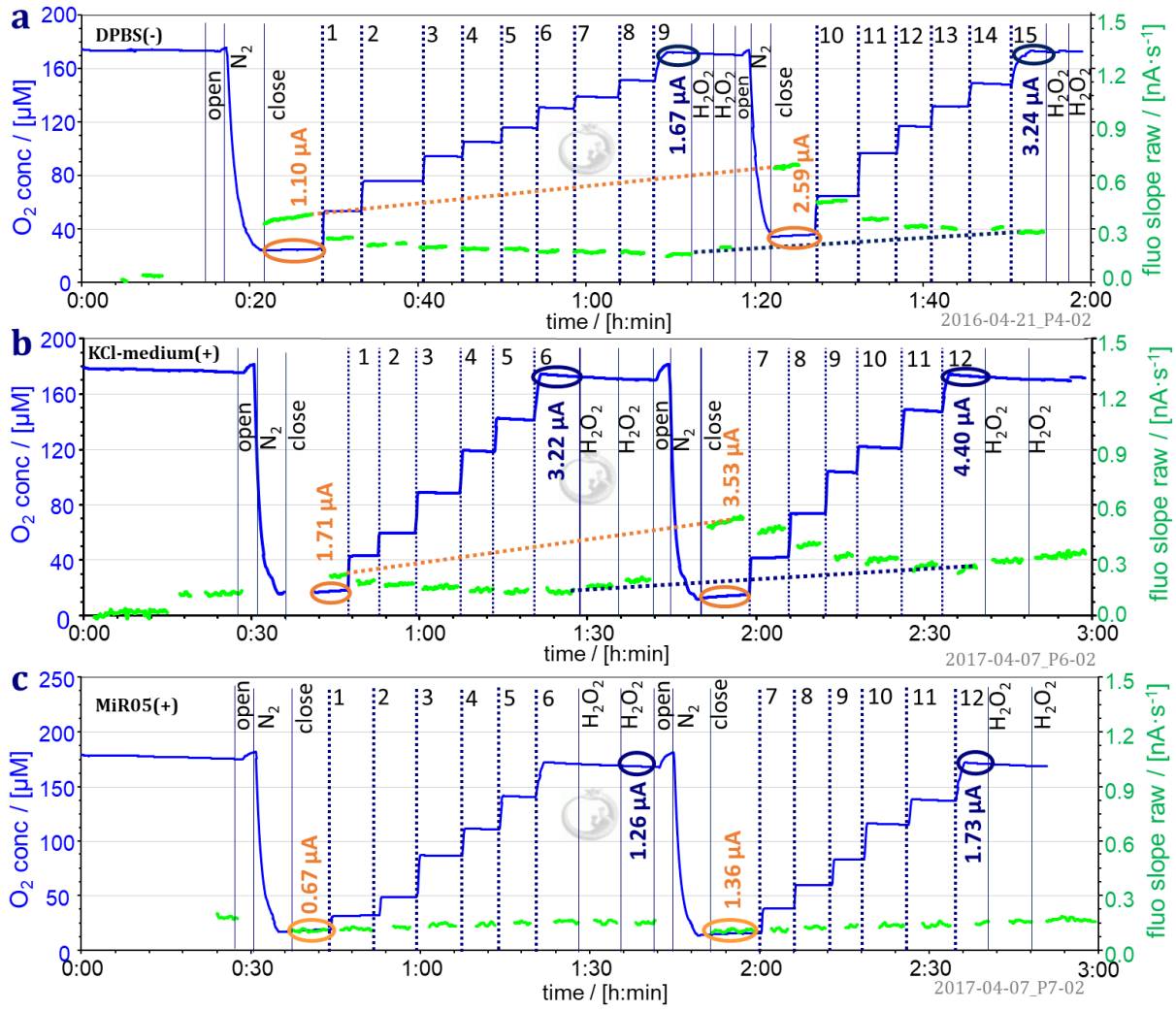

Figure 4. Oxygen dependence of the background fluorescence slope in the Amplex™ UltraRed assay. (a) DPBS(-); **(b)** KCl-medium(+); **(c)** MiR05(+) (see Figure 5c). Blue plots: O_2 concentration [µM] was decreased with N_2 in the gas phase followed by increase of the O_2 concentration in several steps (1 to 15 and 1 to 12). Green plots: background fluorescence slope (raw) [nA·s^{-1}]. The background fluorescence intensity (raw) [µA] is shown at low O_2 concentration (values in orange) and at high O_2 concentration (values in blue). Dotted orange lines: pronounced increase of the apparent H_2O_2 flux at low O_2 concentration as a function of the fluorescence intensity [µA] (values in orange); dotted blue lines: less pronounced increase of the apparent H_2O_2 flux at high O_2 concentration as a function of fluorescence intensity (values in blue).

3.2. Background fluorescence slope as a function of O_2 concentration

To evaluate the contrasting patterns of apparent H_2O_2 flux of yeast observed in different media (Figure 2), we analyzed the background in the absence of yeast as a function of O_2 concentration. The background fluorescence slope is a result of artificial formation of Res (or xRed) independent of the biological sample, which depends on the respiration medium and excitation light intensity (Krumschnabel et al 2015; Zhao et al 2012). We investigated the background fluorescence slope in the AmR assay in DPBS, KCl-medium, and MiR05 at different O_2 concentrations obtained by decreasing the O_2 level by N_2 gas injection followed by stepwise elevation of O_2 concentration up to air-saturation (~ 180 µM; Figure 4). In DPBS and KCl-medium (*1*) the fluorescence slope was high at low O_2 concentration and decreased with increasing O_2 concentration, (*2*) the fluorescence slope increased over time at the same O_2 concentration, and (*3*) the increase of fluorescence intensity over time was more pronounced at low O_2 concentration than at high O_2 concentration (fluorescence signals shown by orange and blue values [µA], respectively, in Figure 4a and b). In MiR05, however, the background fluorescence slope (*1*) increased only slightly from low to high O_2 concentrations, (*2*) did not change over time at the same O_2 concentration, and (*3*) the final fluorescence intensity of 1.7 µA in MiR05 was lower compared to DPBS and KCl-medium (Figure 4c).

We further investigated the fluorescence slope in the AmR assay with DPBS and MiR05 in the absence and presence of yeast (Figures 5 and 6). In DPBS a hyperbolic relationship was observed between the background fluorescence slope and fluorescence intensity (Figure 5a and b). The same pattern was observed at excitation light intensities of 500 mV (Figure 5a) and 250 mV (Figure 5b). The background fluorescence slope increased with decreasing O_2 concentration. Moreover, the hypoxic peaks observed with yeast cells in the reoxygenation cycles matched the pattern of the background fluorescence slope in DPBS (Figure 6a). The hypoxic peaks in the presence of yeast occurred at O_2 concentrations in the range of 5 µM to 10 µM which were below the O_2 levels obtained in the chemical background measurements. This shows that the hypoxic peaks were indistinguishable from the background fluorescence slope in DPBS.

In MiR05 the background fluorescence slope was low compared to DPBS (Figure 5a and c). An increase of the background fluorescence slope with fluorescence intensity becomes apparent at enlarged scales, but the O_2 concentration exerted only a subtle effect on the background fluorescence slope (zoom in Figure 5d). The fluorescence slope measured in the presence of yeast at high O_2 concentrations was higher than the background fluorescence slope and it decreased at low O_2 levels overlapping with the background fluorescence slope (Figure 6b and c). The background-corrected fluorescence slopes, therefore, indicate a decline of extracellular H_2O_2 flux from high to low O_2 concentration.

3.3. Background correction

In DPBS, the high background fluorescence slope overlapping with the experimental fluorescence slope in the presence of yeast made it impossible to apply a meaningful background correction.

For experiments in MiR05, we calculated the background flux $J_{amp,BG}$ applying the following step-wise background corrections.

1. Linear dependence on fluorescence intensity I_{amp} [µA] measured at the reference O_2 concentration $[O_2]_r$ which was close to air saturation (Figure 1e, Table 2).
2. Linear dependence on O_2 concentration (Figure 6b and c) described by the oxygen correction factor F_{O2}. $[O_2]_e$ is the experimental O_2 concentration at a given respiratory state,

$$F_{O2}=(0.0002\cdot [O_2]_e+0.067)/(0.0002\cdot[O_2]_r+0.067) \quad \text{Eq.2}$$

3. Oxygen-adjusted background fluorescence slope $J_{amp,BG}$ [nA·s^{-1}],

$$J_{amp,BG} = J_{amp,BGr}\cdot F_{O2} \quad \text{Eq.3}$$

4. Background-corrected experimental fluorescence slope $J_{amp,corr}$ [nA·s^{-1}] based on the experimental fluorescence slope in the presence of sample J_{amp} [nA·s^{-1}] at $[O_2]_e$,

$$J_{amp,corr} = J_{amp} - J_{amp,BG} \quad \text{Eq.4}$$

5. Calibration for H_2O_2-sensitivity [µA·µM^{-1}] determined from H_2O_2 calibrations (Komlódi et al 2018) to obtain extracellular H_2O_2 flux J_{H2O2} [pmol·s^{-1}·mL^{-1}],

$$J_{H2O2} = J_{amp,corr} / \text{sensitivity} \quad \text{Eq.5}$$

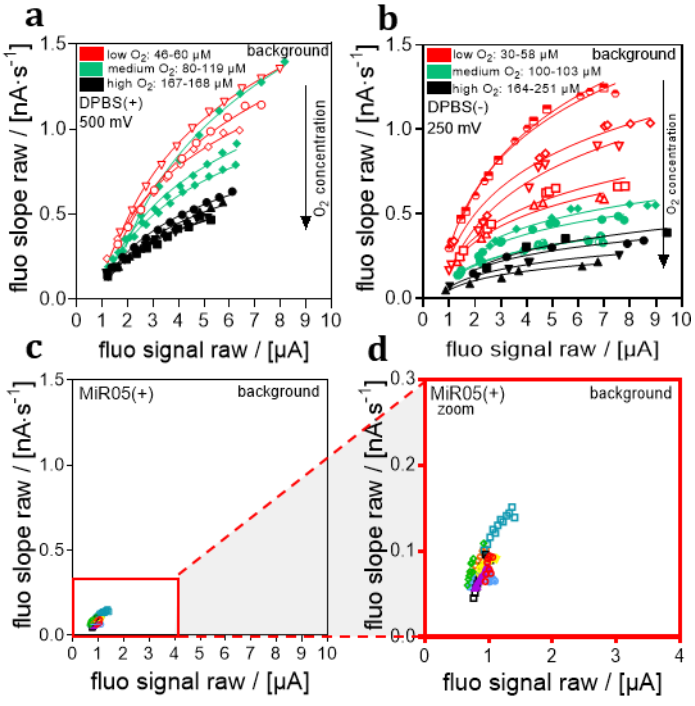

Figure 5. Oxygen dependence of the background fluorescence slope (apparent H_2O_2 flux without yeast) as a function of fluorescence signal [µA] (proportional to fluorescence intensity) in DPBS and MiR05. Background fluorescence slope (raw) [nA·s^{-1}] as a function of fluorescence signal. **(a)** DPBS(+), excitation light intensity 500 mV; ten different O2k-chambers (n=10, five O2k). Lines are fitted by nonlinear regression; r^2=0.95-0.99. **(b)** DPBS(-) without DTPA, excitation light intensity 250 mV; 14 different O2k-chambers (n=14, seven O2k); r^2=0.95-0.99. For DPBS, colors indicate measurements at constant O_2 concentrations (shown by numbers [µM]) measured at fluorescence intensities increasing over time. **(c)** MiR05(+), excitation light intensity 500 mV; O_2 concentrations changed from ~ 20 µM to air saturation in the same experimental run (representative trace in Figure 4c). Each colour represents a technical repeat (n=8). **(d)** Zoom into panel **c**.

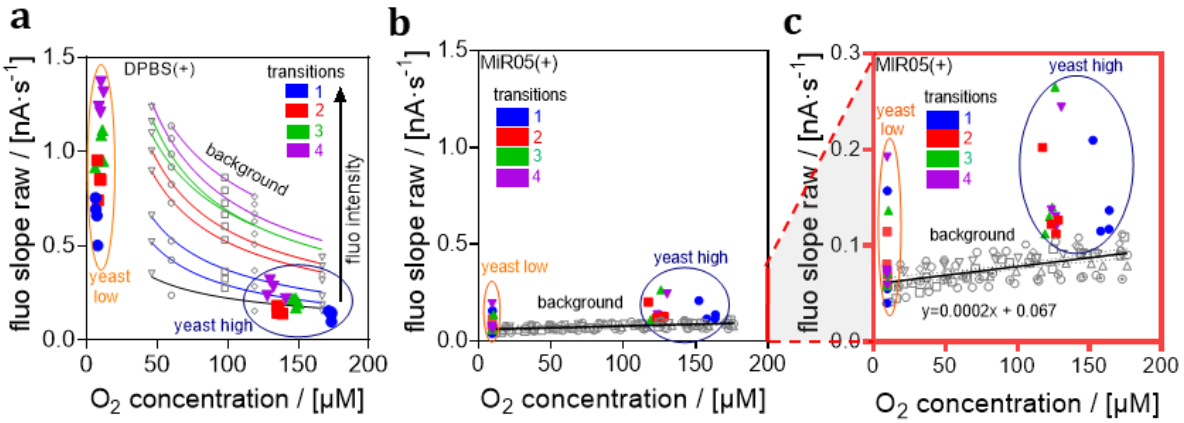

Figure 6. Fluorescence slope (apparent H_2O_2 flux with or without yeast) as a function of oxygen concentration in DPBS and MiR05. Non-calibrated fluorescence slope [nA·s^{-1}] in background (without yeast; open grey symbols) and in the presence of yeast in the reoxygenation cycles with transitions from high to low O_2 concentrations (closed symbols; enclosed by blue and orange outlines, respectively). Identical colors of symbols indicate technical repeats (n=4). Different colors of symbols distinguish the first to fourth transitions (1 to 4). **(a)** DPBS(+) background (from Figure 5a). Lines are fitted by nonlinear regression through data points at constant fluorescence signal; r^2=0.96-0.99. Different colors of lines reflect the pattern of fluorescence intensity measured in the reoxygenation cycles with yeast (from Figure 2d; peak fluorescence at low O_2 concentrations). **(b)** MiR05(+) background (from Figure 1e). Line is fitted by linear regression; r^2=0.80. **(c)** Zoom into panel **b**.

Table 2. Background parameters for different Lots of MiR05-Kit. Assays with DTPA. Slope b_{amp} and intercept a_{amp} (Eq.1; Materials and methods).

Lot #	b_{amp}	a_{amp}
0915	0.0082	0.1159
18.02872	-0.0198	0.0914
19.01689	-0.0116	0.0868
20J01923	-0.0348	0.1248

3.4. O_2 kinetics of H_2O_2 flux and O_2 flux

O_2 consumption and xRed fluorescence slope (apparent H_2O_2 flux) were measured simultaneously in repeated normoxic-anoxic transitions in yeast cells in MiR05 and DPBS (Figure 7). During the first transition the cells acclimatized to experimental conditions immediately after rehydration. At normoxic O_2 concentration yeast respiration stabilized during the following reoxygenation cycles (Figure 2a, 2c and 3). Therefore, we analysed the second transitions (Figure 7a and b).

Respiration was a complex function of O_2 concentration in the high O_2 regime including factors of time and non-mitochondrial O_2 consumption (Gnaiger et al 1995). A zoom into the low O_2 range reveals first-order hyperbolic kinetics (Figure 7c). The

maximum kinetic O_2 flux (J_{max}) varied as a function of respiration media and the number of normoxic-anoxic transitions (experimental exposure time). J_{max} was calculated as a parameter of the hyperbolic fit indicating O_2 flux at high, non-limiting O_2 concentrations (see Materials and methods). The p_{50} was about four times higher than the p_{50} of isolated mitochondria and small mammalian cells, indicating the effect of intracellular diffusion gradients in the yeast cells (Gnaiger 2003; Scandurra, Gnaiger 2010). c_{50} (p_{50}) varied as a function of J_{max} (Figure 7d) consistent with the concept of kinetic electron trapping by cytochrome *c* oxidase (Verkhovsky et al 1996; Gnaiger 2001). This indicates that the incubation medium did not exert any specific effect on respiratory O_2 kinetics. In contrast, there was a dramatic difference in the dependence of apparent H_2O_2 flux on O_2 concentration in different media. In DPBS a sharp hypoxic peak of J_{amp} was observed at low O_2 concentration (uncorrected; Figure 7b). In MiR05, however, background-corrected J_{H2O2} remained low and was a linear function of O_2 concentration in the normoxic to hypoxic range (Figure 7a). A higher resolution of H_2O_2 flux was obtained in a separate batch of yeast which showed increased respiration and H_2O_2 flux near air saturation (Figure 8). The H_2O_2 flux was a biphasic function of O_2 concentration, with a linear decline in the normoxic to hypoxic range and a steep decline of H_2O_2 flux in the microoxic range when respiration was limited by O_2 concentration.

4. Discussion

H_2O_2 flux of yeast in MiR05 was linearly dependent on O_2 concentration; H_2O_2 flux did not increase at low O_2 concentration even after multiple normoxic-anoxic transitions (Figure 2 and 8). This observation is in line with studies on mammalian mitochondria by Boveris and Chance (1973), Duong et al (2020), Li Puma et al (2020), Robb et al (2018), Stepanova et al (2017, 2018a, 2018b, 2020), and Szibor et al (2020) showing a linear increase of H_2O_2 production with O_2 concentration. These results contrast with the concept of reductive stress and elevated hypoxic H_2O_2 generation (Chandel et al 1998; Guzy et al 2007; Hernansanz-Augustin et al 2014; Waypa et al 2001). The viability of CuZnSOD null mutants of *S. cerevisiae* is compromised at normoxia but not at low aeration levels (Longo et al 1996), consistent with decreased ROS production under hypoxia corresponding to intracellular oxygen pressures of mammalian cells in tissues.

Besides H_2O_2-independent formation of xRed (or Res), several potential methodological artefacts are discussed in the literature related to the metabolites or enzyme activities in the biological sample. (*1*) Res can undergo a one-electron reduction to form a semiquinoneimine-type radical which regenerates AmR and superoxide anion by NADPH-cytochrome P450 reductase in liver microsomes (Dutton et al 1989). (*2*) Complex I can initiate cycling of oxidized and reduced Res in the presence of NADH and other reductants (Grivennikova et al 2018). (*3*) HRP can catalyze the oxidation of Res in the presence of peroxynitrite, and peroxynitrite-derived radicals can oxidize AmR to Res (Dębski et al 2016). (*4*) In liver and kidney, AmR can be converted to Res/xRed by mt-carboxylesterases mtCES which can be prevented using mtCES inhibitors such as phenylmethyl sulfonyl fluoride (Miwa et al 2015). If AmR does not cross the cell wall and plasma membrane of yeast cells, these side-effects can be excluded in our experiments. If, however, AmR reacts with intracellular carboxylesterases, this would not explain the

absence of the hypoxic peak in MiR05 (Figure 8) nor the induction of the hypoxic peak in DPBS at high fluorescence intensity (Figure 3). We added SOD to all AmR assays to not only convert superoxide to H_2O_2 and O_2 but to minimize formation of Res (or xRed) in a photosensitized reaction with NADH and reduced glutathione (Votyakova and Reynold 2004; Zhao et al 2011, 2012).

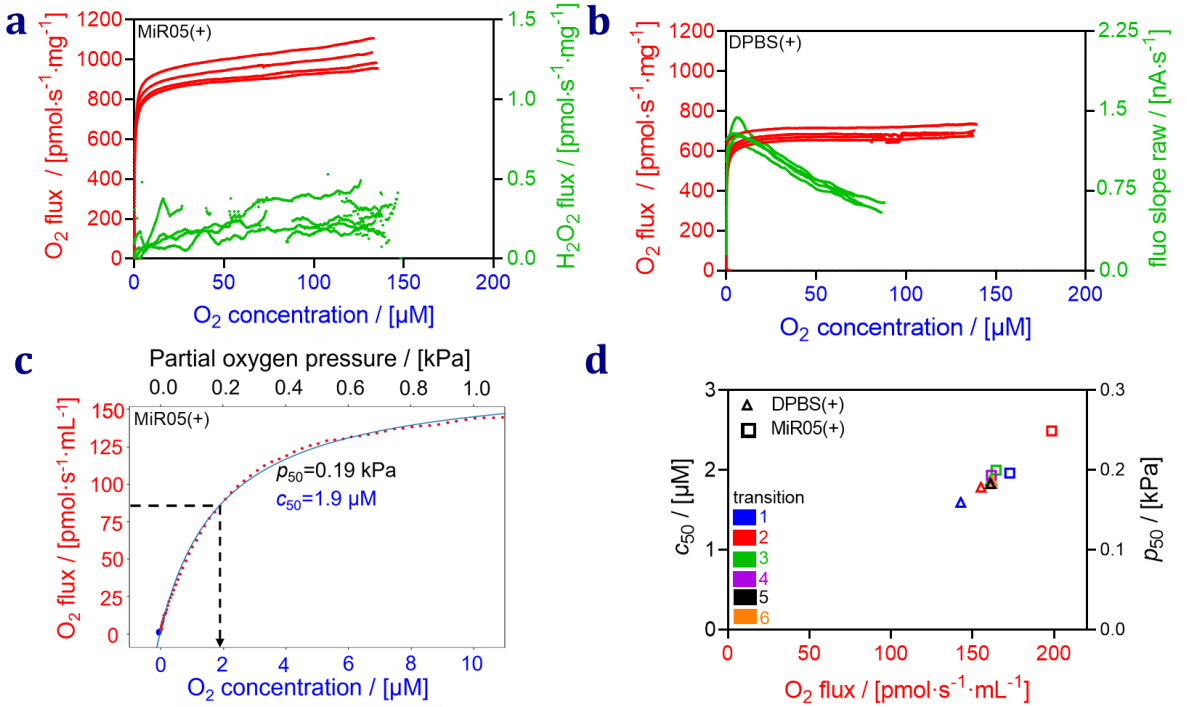

Figure 7. O_2 flux and H_2O_2 flux as a function of O_2 concentration in yeast cells (37 °C). (a) MiR05(+); **(b)** DPBS(+); second normoxic-anoxic transitions in the ROUTINE state (n=4). Data are from Figure 2d and f. Red plots: mass-specific O_2 flux [pmol·s^{-1}·mg^{-1}]; **(a)** green plots: H_2O_2 flux is shown after H_2O_2 calibration performed at ~ 150 µM O_2; **(b)** fluorescence slope J_{amp}; **(c)** O_2 kinetic plot of respiration with zoom into the low O_2 concentration range. Volume-specific O_2 flux $J_{V,O2}$ [pmol·s^{-1}·mL^{-1}] as a function of O_2 concentration and partial oxygen pressure p_{O2} [kPa] in MiR05. Dots show individual data points measured at 2-s time intervals. Blue line: hyperbolic fit. Experiment 2018-12-06_P4-02A from Figure 2c, second transition. **(d)** c_{50} [µM] and p_{50} [kPa] as a function of maximum volume-specific O_2 flux J_{max} at identical yeast concentrations in MiR05 and DPBS for the first to fourth transitions. Colors distinguish peaks (1 to 6) in the first to sixth transitions.

In the present study we investigated the O_2 dependence of extracellular H_2O_2 flux in yeast. In DPBS and KCl-medium, a hypoxic peak was observed at low O_2 concentration, which increased with the sequential number of reoxygenations and normoxic-anoxic transitions. Theoretically this increase of the fluorescence slope might indicate H_2O_2 formation triggered by reductive stress at low O_2 concentrations and hypoxic preconditioning (Hernansanz-Agustín et al 2014; Smith et al 2017). However, the hypoxic peak could be explained entirely by the background fluorescence slope. The hypoxic peak

is a methodological artefact caused by autooxidation of AmR at increasing fluorescence intensity and under hypoxia in the range of 5 µM to 10 µM O_2 corresponding to 2.5 % to 5 % air saturation (Figure 9).

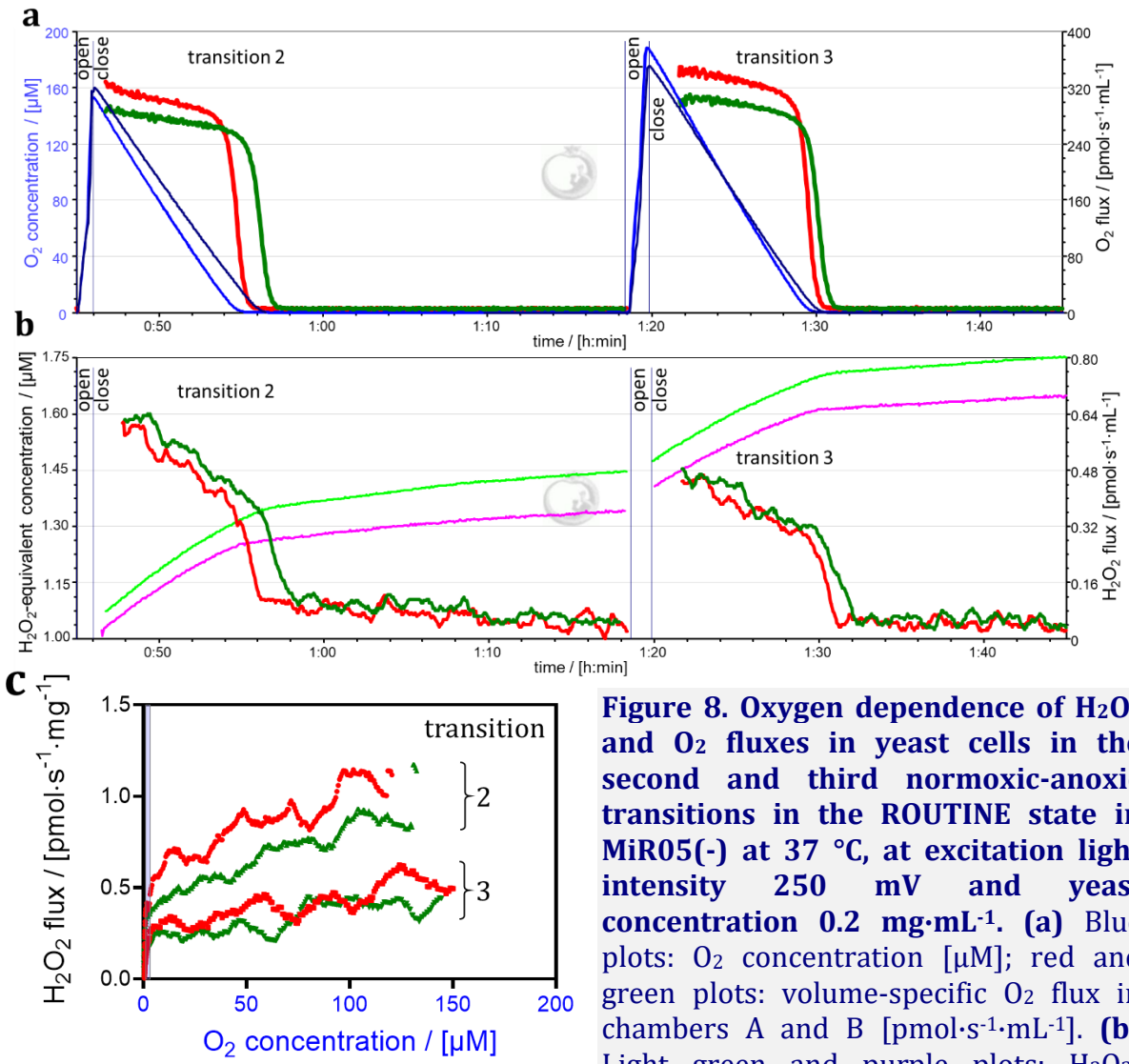

Figure 8. Oxygen dependence of H_2O_2 and O_2 fluxes in yeast cells in the second and third normoxic-anoxic transitions in the ROUTINE state in MiR05(-) at 37 °C, at excitation light intensity 250 mV and yeast concentration 0.2 mg·mL^{-1}. (a) Blue plots: O_2 concentration [µM]; red and green plots: volume-specific O_2 flux in chambers A and B [pmol·s^{-1}·mL^{-1}]. **(b)** Light green and purple plots: H_2O_2-equivalent concentration [µM]; red and green plots: volume-specific H_2O_2 flux [pmol·s^{-1}·mL^{-1}] in chambers A and B. **(c)** Mass-specific H_2O_2 flux [pmol·s^{-1}·mg^{-1}] from panel **b** corrected for background fluorescence slope. Shaded area indicates the low-oxygen range when respiration declined as a hyperbolic function of oxygen (Figure 7). Experiment 2016-03-03_P12-02.

MiR05 is optimized for assessment of mitochondrial respiration during prolonged incubation times to preserve mitochondrial function (Gnaiger et al 2000). The sensitivity of the AmR assay is more stable in MiR05 than in DPBS, KCl-medium, and buffer Z in experiments up to 2 h (Komlódi et al 2018). This was confirmed in the present background experiments at air saturation (Figure 1). Importantly, MiR05 prevented the

artefact of the hypoxic peak (Figures 4 to 6). This might be explained by the high antioxidant capacity of MiR05 (Figure 9). However, preliminary results suggest that the artefact of the hypoxic peak does neither occur in 50 mM phosphate buffer, at higher yeast concentration (1.5 mg/mL), low excitation light intensity (100 mV), and lower temperature (28 °C; Supplement Figure S1).

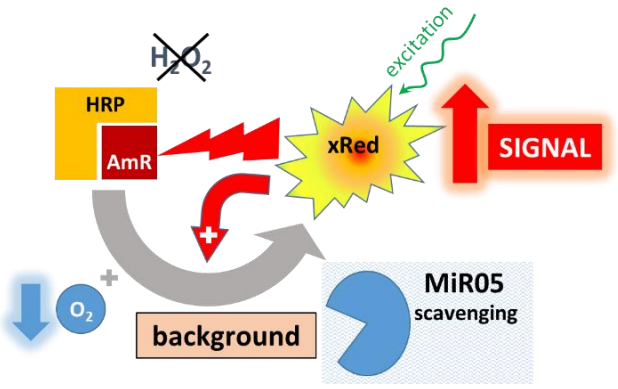

Figure 9. UltroxRed (xRed) formation in H_2O_2-independent reactions in the absence of biological sample. xRed is formed in the absence of H_2O_2 in the AmR-HRP reaction contributing to the background fluorescence slope. Excitation light can initiate xRed generation which induces further xRed formation via photooxidation of AmR in a self-amplification process. These phenomena and the decrease of O_2 concentration result in the increase of the background fluorescence signal which is scavenged by the antioxidants in MiR05 thus preventing the hypoxic peak.

In agreement with Li Puma et al (2020), a linear relationship was observed between O_2 concentration and background fluorescence slope in the AmR assay measured in MiR05. This provides the basis for correction for background fluorescence slope and evaluation of the O_2 dependence of H_2O_2 flux not only in yeast but generally in applications of the AmR assay in living and permeabilized cells, and isolated mitochondria including mammalian cell models.

Conclusions

In studies of H_2O_2 flux as a function of O_2 concentration using the AmR assay, the respiration medium MiR05 offers advantages compared with DPBS and KCl-medium. An apparent maximum of H_2O_2 production under hypoxia was explained as chemical background-related artefact in DPBS and KCl-medium. The background fluorescence slope and its O_2 dependence are minimized in MiR05, allowing for accurate background correction. Under these conditions, extracellular H_2O_2 flux of living yeast showed a biphasic oxygen dependence. H_2O_2 flux decreased abruptly towards anoxia when respiration showed a hyperbolic dependence on O_2 concentration. Above this critical O_2 concentration, H_2O_2 flux increased linearly from hypoxia to hyperoxia at constant respiration, which does not support the concept of reductive stress.

Acknowledgements

We thank Manuela Passrugger, Marco Di Marcello for excellent technical support in buffer preparation, and maintenance of the O2ks, Marco Di Marcello for analysis of the p_{50} data, and Carolina Doerrier for valuable comments on the manuscript. This work was partially funded by project NextGen-O2k which has received funding from the European Union's Horizon 2020 research and innovation programme under grant agreement Nº 859770. Ondrej Sobotka´s secondments were founded by PROGRES Q40/02.

Abbreviations

a_{amp}	intercept
AmR	Amplex™ UltraRed
b_{amp}	slope
DPBS	Dulbecco´s Phosphate Buffered Saline
DCFH	2´,7´-dichlorofluorescein
DHE	dihydroethidine
DTPA	diethylentriamin-*N*,*N*,*N*',*N*'',*N*'''-pentaacetic acid
c_{50}	oxygen concentration at which respiratory flux is 50 % of J_{max}
ETS	electron transfer system
F_{O2}	oxygen correction factor
HRP	horseradish peroxidase
H_2O_2	hydrogen peroxide
J_{amp}	experimental fluorescence slope
$J_{amp,BG}$	oxygen-adjusted background fluorescence slope
$J_{amp,BGr}$	raw background fluorescence slope
$J_{amp,corr}$	background-corrected experimental fluorescence slope
J_{H2O2}	hydrogen peroxide flux
J_{max}	maximum volume-specific oxygen flux
$J_{V,O2}$	volume-specific oxygen flux
I_{amp}	fluorescence intensity
KCl	potassium-chloride
mtCES	mt-carboxylesterases
$[O_2]_e$	experimental oxygen concentration
$[O_2]_r$	reference oxygen concentration
p	oxygen partial pressure [kPa]
p_{50}	oxygen partial pressure at which respiratory flux is 50 % of J_{max}
Res	resorufin
ROS	reactive oxygen species
SOD	superoxide dismutase
xRed	UltroxRed

References

Aon MA, Cortassa S, O'Rourke B (2010) Redox-optimized ROS balance: a unifying hypothesis. Biochim Biophys Acta 1797:865-77.

Bienert GP, Schjoerring JK, Jahn TP (2006) Membrane transport of hydrogen peroxide. Biochim Biophys Acta 1758:994-1003.

Boveris A, Chance B (1973) The mitochondrial generation of hydrogen peroxide. General properties and effect of hyperbaric oxygen. Biochem J 134:707-16.

Brand MD (2016) Mitochondrial generation of superoxide and hydrogen peroxide as the source of mitochondrial redox signaling. Free Radical Biol Med 100:14-31.

Buettner GR, Wagner BA, Rodgers VG (2013) Quantitative redox biology: an approach to understand the role of reactive species in defining the cellular redox environment. Cell Biochem Biophys 67:477-83.

Chandel NS, Maltepe E, Goldwasser E, Mathieu CE, Simon MC, Schumacker PT (1998) Mitochondrial reactive oxygen species trigger hypoxia-induced transcription. Proc Natl Acad Sci 95:11715-20.

Crowe HJ, Carpenter FJ, Crowe M (1998) The role of vitrification in anhydrobiosis. Annu Rev Physiol 60:73-103.

Dawson TL, Gores GJ, Nieminen AL, Herman B, Lemasters JJ (1993) Mitochondria as a source of reactive oxygen species during reductive stress in rat hepatocytes. Am J Physiol 264:C961-7.

Dębski D, Smulik R, Zielonka J, Michałowski B, Jakubowska M, Dębowska K, Adamus J, Marcinek A, Kalyanaraman B, Sikora A (2016) Mechanism of oxidative conversion of Amplex® Red to resorufin: pulse radiolysis and enzymatic studies. Free Radic Biol Med 95:323-32.

Dikalov SI, Harrison DG (2014) Methods for detection of mitochondrial and cellular reactive oxygen species. Antioxid Redox Signal 20:372–82.

Doerrier C, Garcia-Souza LF, Krumschnabel G, Wohlfarter Y, Mészáros AT, Gnaiger E (2018) High-Resolution FluoRespirometry and OXPHOS protocols for human cells, permeabilized fibers from small biopsies of muscle, and isolated mitochondria. Methods Mol Biol 1782:31-70.

Duong QV, Hoffman A, Zhong K, Dessinger MJ, Zhang Y, Bazil JN (2020) Calcium overload decreases net free radical emission in cardiac mitochondria. Mitochondrion 51:126-39.

Dutton DR, Reed GA, Parkinson A (1989) Redox cycling of resorufin catalyzed by rat liver microsomal NADPH-cytochrome P450 reductase. Arch Biochem Biophys 268:605-16.

Gnaiger E (2001) Bioenergetics at low oxygen: dependence of respiration and phosphorylation on oxygen and adenosine diphosphate supply. Respir Physiol 128:277-97.

Gnaiger E (2003) Oxygen conformance of cellular respiration. A perspective of mitochondrial physiology. Adv Exp Med Biol 543:39-55.

Gnaiger E (2008) Polarographic oxygen sensors, the oxygraph and high-resolution respirometry to assess mitochondrial function. In: Mitochondrial dysfunction in drug-induced toxicity (Dykens JA, Will Y, eds) John Wiley & Sons, Inc, Hoboken, NJ:327-52.

Gnaiger E, Kuznetsov AV, Schneeberger S, Seiler R, Brandacher G, Steurer W, Margreiter R (2000) Mitochondria in the cold. In: Life in the Cold (Heldmaier G, Klingenspor M, eds) Springer, Berlin, Heidelberg:431-42.

Gnaiger E, Steinlechner-Maran R, Méndez G, Eberl T, Margreiter R (1995) Control of mitochondrial and cellular respiration by oxygen. J Bioenerg Biomembr 27:583-96.

Grivennikova VG, Kareyeva AV, Vinogradov AD (2018) Oxygen-dependence of mitochondrial ROS production as detected by Amplex Red assay. Redox Biol 17:192-9.

Guzy RD, Mack MM, Schumacker PT (2007) Mitochondrial complex III is required for hypoxia-induced ROS production and gene transcription in yeast. Antioxid Redox Signal 9:1317-28.

Hernansanz-Agustín P, Izquierdo-Álvarez A, Sánchez-Gómez FJ, Ramos E, Villa-Piña T, Lamas S, Bogdanova A, Martínez-Ruiz A (2014) Acute hypoxia produces a superoxide burst in cells. Free Radic Biol Med 71:146-56.

Hoffman DL, Salter JD, Brookes PS (2007) Response of mitochondrial reactive oxygen species generation to steady-state oxygen tension: implications for hypoxic cell signaling. Am J Physiol Heart Circ Physiol 292:H101-8.

Kalyanaraman B, Darley-Usmar V, Davies KJA, Dennery PA, Forman HJ, Grisham MB, Mann GE, Moore K, Roberts LJ 2nd, Ischiropoulos H (2012) Measuring reactive oxygen and nitrogen species with fluorescent probes: challenges and limitations. Free Radical Biol Med 52:1-6.

Koga S, Echigo A, Nunomura K (1966) Physical properties of cell water in partially dried *Saccharomyces cerevisiae*. Biophys J 6:665-74.

Komlódi T, Sobotka O, Krumschnabel G, Bezuidenhout N, Hiller E, Doerrier C, Gnaiger E (2018) Comparison of mitochondrial incubation media for measurement of respiration and hydrogen peroxide production. Methods Mol Biol 1782:137-55.

Korge P, Calmettes G, Weiss JN (2015) Increased reactive oxygen species production during reductive stress: the roles of mitochondrial glutathione and thioredoxin reductases. Biochim Biophys Acta 1847:514–25.

Krumschnabel G, Fontana-Ayoub M, Sumbalova Z, Heidler J, Gauper K, Fasching M, Gnaiger E (2015) Simultaneous high-resolution measurement of mitochondrial respiration and hydrogen peroxide production. Methods Mol Biol 1264:245-61.

Li Puma LC, Hedges M, Heckman JM, Mathias AB, Engstrom MR, Brown AB, Chicco AJ (2020) Experimental oxygen concentration influences rates of mitochondrial hydrogen peroxide release from cardiac and skeletal muscle preparations. Am J Physiol Regul Integr Comp Physiol 318:R972-80.

Longo VD, Gralla EB, Valentine JS (1996) Superoxide dismutase activity is essential for stationary phase survival in *Saccharomyces cerevisiae*. Mitochondrial production of toxic oxygen species in vivo. J Biol Chem 271:12275-80.

Makrecka-Kuka M, Krumschnabel G, Gnaiger E (2015) High-resolution respirometry for simultaneous measurement of oxygen and hydrogen peroxide fluxes in permeabilized cells, tissue homogenate and isolated mitochondria. Biomolecules 5:1319-38.

Mishin V, Gray JP, Heck DE, Laskin DL, Laskin JD (2010) Application of the Amplex red/horseradish peroxidase assay to measure hydrogen peroxide generation by recombinant microsomal enzymes. Free Radic Biol Med 48:1485-91.

Miwa S, Treumann A, Bell A, Vistoli G, Nelson G, Hay S, von Zglinicki T (2015) Carboxylesterase converts Amplex red to resorufin: Implications for mitochondrial H_2O_2 release assays. Free Radic Biol Med 90:173-83.

Mohanty JG, Jaffe JS, Schulman ES, Raible DG (1997) A highly sensitive fluorescent micro-assay of H_2O_2 release from activated human leukocytes using a dihydroxyphenoxazine derivative. J Immunol Meth 202:133-41.

Ottolenghi S, Sabbatini G, Brizzolari A, Samaja M, Chiumello D (2020) Hyperoxia and oxidative stress in anesthesia and critical care medicine. Minerva Anestesiol 86:64-75.

Paniker NV, Srivastava SK, Beutler E (1970) Glutathione metabolism of the red cells. Effect of glutathione reductase deficiency on the stimulation of hexose monophosphate shunt under oxidative stress. Biochim Biophys Acta 215:456-60.

Piwonski HM, Goomanovsky M, Bensimon D, Horovitz A, Haran G (2012) Allosteric inhibition of individual enzyme molecules trapped in lipid vesicles. Proc Natl Acad Sci U S A 109:E1437-43.

Robb EL, Hall AR, Prime TA, Eaton S, Szibor M, Viscomi C, James AM, Murphy MP (2018) Control of mitochondrial superoxide production by reverse electron transport at complex I. J Biol Chem 293:9869-79.

Scandurra FM, Gnaiger E (2010) Cell respiration under hypoxia: facts and artefacts in mitochondrial oxygen kinetics. Adv Exp Med Biol 662:7-25.

Sies H (1997) Oxidative stress: oxidants and antioxidants. Exp Physiol 82:291-5.

Sies H, Jones DP (2020) Reactive oxygen species (ROS) as pleiotropic physiological signalling agents. Nat Rev Mol Cell Biol 21:363-83.

Skulachev VP (1996) Role of uncoupled and non-coupled oxidations in maintenance of safely low levels of oxygen and its one-electron reductants. Q Rev Biophys 29:169-202.

Smith KA, Waypa GB, Schumacker PT (2017) Redox signaling during hypoxia in mammalian cells. Redox Biol 13:228-34.

Stepanova A, Kahl A, Konrad C, Ten V, Starkov AS, Galkin A (2017) Reverse electron transfer results in a loss of flavin from mitochondrial complex I: Potential mechanism for brain ischemia-reperfusion injury. J Cereb Blood Flow Metab 37:3649-58.

Stepanova A, Konrad C, Guerrero-Castillo S, Manfredi G, Vannucci S, Arnold S, Galkin A (2018a) Deactivation of mitochondrial complex I after hypoxia-ischemia in the immature brain. J Cereb Blood Flow Metab 39:1790-802.

Stepanova A, Konrad C, Manfredi G, Springett R, Ten V, Galkin A (2018b) The dependence of brain mitochondria reactive oxygen species production on oxygen level is linear, except when inhibited by antimycin A. J Neurochem 148:731-45.

Stepanova A, Galkin A (2020) Measurement of mitochondrial H_2O_2 production under varying O_2 tensions. Methods Cell Biol 155:273-93.

Szibor M, Schreckenberg R, Gizatullina Z, Dufour E, Wiesnet M, Dhandapani PK, Debska-Vielhaber G, Heidler J, Wittig I, Nyman TA, Gaertner U, Hall AR, Pell V, Viscomi C, Krieg T, Murphy MP, Braun T, Gellerich FN, Schlueter KD, Jacobs HT (2020) Respiratory chain signalling is essential for adaptive remodelling following cardiac ischaemia. J Cell Mol Med 24:3534-48.

Tretter L, Ambrus A (2014) Measurement of ROS homeostasis in isolated mitochondria. Methods Enzymol 547:199-223.

Verkhovsky MI, Morgan JE, Puustein A, Wikström M (1996) Kinetic trapping of oxygen in cell respiration. Nature 380:268-70.

Votyakova TV, Reynolds IJ (2004) Detection of hydrogen peroxide with Amplex Red: interference by NADH and reduced glutathione auto-oxidation. Arch Biochem Biophys 431:138-44.

Waypa GB, Chandel NS, Schumacker PT (2001) Model for Hypoxic Pulmonary Vasoconstriction Involving Mitochondrial Oxygen Sensing. Circ Res 88:1259–1266.

Xiao W, Loscalzo J (2020) Metabolic responses to reductive stress. Antioxid Redox Signal 32:1330-47.

Zhao B, Ranguelova K, Jiang J, Mason RP (2011) Studies on the photosensitized reduction of resorufin and implications for the detection of oxidative stress with Amplex Red. Free Radic Biol Med 51:153-9.

Zhao B, Summers FA, Mason RP (2012) Photooxidation of Amplex Red to resorufin: implications of exposing the Amplex Red assay to light. Free Radical Biol Med 51: 153–9.

Zhou M, Diwu Z, Panchuk-Voloshina N, Haugland RP (1997) A stable nonfluorescent derivative of resorufin for the fluorometric determination of trace hydrogen peroxide: applications in detecting the activity of phagocyte NADPH oxidase and other oxidases. Anal Biochem 253:162-8.

Supplement

Respiration of freeze-dried yeast suspended in 50 mM Na-phosphate buffer was stimulated by extracellular glucose (Figure S1a). Subsequently, respiration further doubled upon stimulation by ethanol and uncoupler titrations (not shown). These additions exerted a minor effect on extracellular H_2O_2 production, which was a linear function of environmental oxygen concentration in the hypoxic to hyperoxic range (Figure S1b and c). The biphasic oxygen dependence of H_2O_2 flux obtained in Na-phosphate buffer was comparable with results in MiR05 (Figure 8).

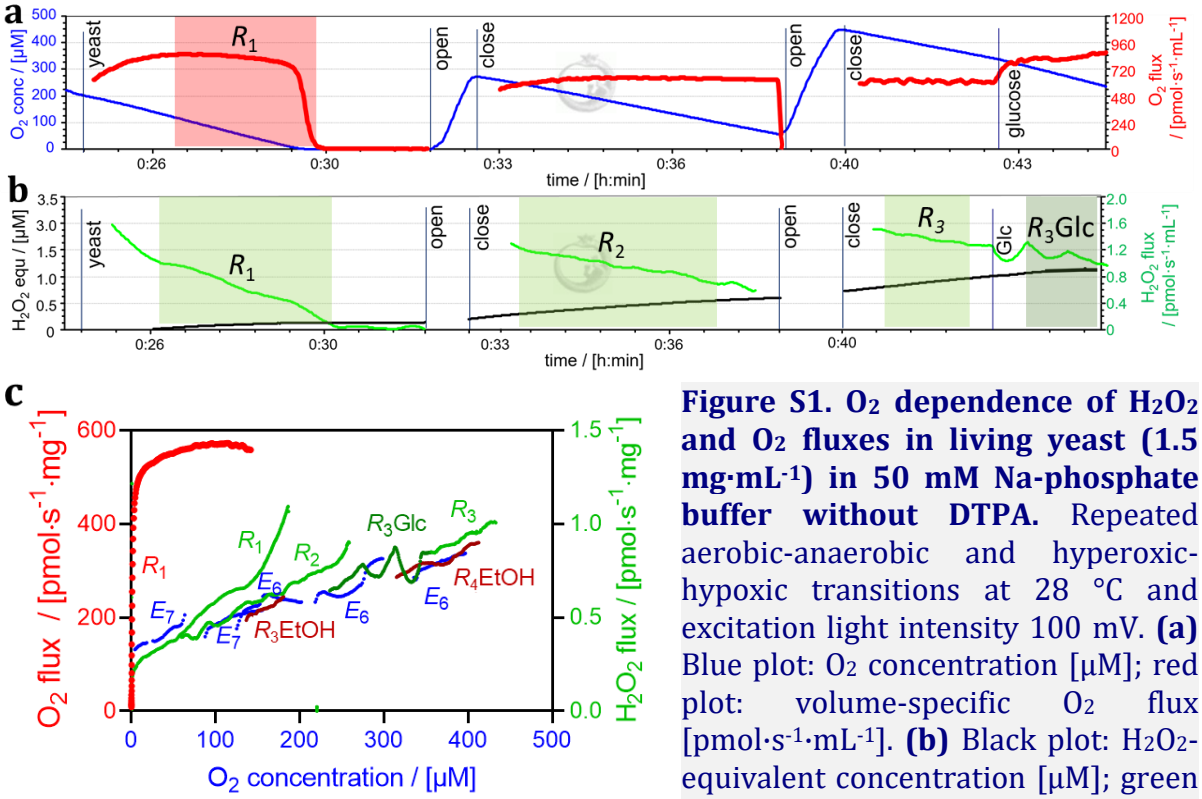

Figure S1. O_2 dependence of H_2O_2 and O_2 fluxes in living yeast (1.5 mg·mL^{-1}) in 50 mM Na-phosphate buffer without DTPA. Repeated aerobic-anaerobic and hyperoxic-hypoxic transitions at 28 °C and excitation light intensity 100 mV. **(a)** Blue plot: O_2 concentration [µM]; red plot: volume-specific O_2 flux [pmol·s^{-1}·mL^{-1}]. **(b)** Black plot: H_2O_2-equivalent concentration [µM]; green plot: volume-specific H_2O_2 flux [pmol·s^{-1}·mL^{-1}]. **(c)** Mass-specific O_2 flux [pmol·s^{-1}·mg^{-1}] from panel **a** in the first reoxygenation cycle (R_1), and biphasic oxygen dependence of mass-specific H_2O_2 flux [pmol·s^{-1}·mg^{-1}] from panel **b** in the first, second and third reoxygenation cycles in the ROUTINE state (R_1, R_2, R_3), after glucose (20 mM) addition in the third reoxygenation cycle (R_3Glc), after ethanol (20 µL/mL) addition in the third (R_3EtOH) and fourth (R_4EtOH) reoxygenation, after uncoupler titration (2.5 to 30 µM carbonyl cyanide p-trifluoro-methoxyphenyl hydrazone FCCP) in the sixth (E_6) and seventh reoxygenation (E_7). Experiment 2012-03-20_EF-02A.